Available online at www.sciencedirect.com

ScienceDirect

Procedia CIRP 78 (2018) 382–387

www.elsevier.com/locate/procedia

6th CIRP Global Web Conference
"Envisaging the future manufacturing, design, technologies and systems in innovation era"

Design criteria for grinding machine dynamic stability

Marco Leonesio[a]*, Giacomo Bianchi[a], Nicola Cau[b]

[a]*CNR – STIIMA, Institute of Intelligent Industrial Technologies and Systems for Advanced Manufacturing - National Research Council of Italy, Via Corti 12, 20133 Milan, Italy*
[b]*PhiDrive s.r.l., Via Bolzano, 1/E, 20871 Vimercate (MB), Italy*

* Corresponding author. Tel.: +39 0223699952; fax: +39 0223699941. *E-mail address:* marco.leonesio@itia.cnr.it

Abstract

Surface grinding is one of the oldest and most widely used machining process: to date, there are still few alternatives available for producing smooth and flat surfaces, satisfying both technical and economic constraints. The quality of a workpiece resulting from a grinding process is strongly influenced by the static and dynamic behavior of the mechanical system, composed by machine tool, wheel, fixture and workpiece. In particular, the dynamic compliance of the machine at wheel-workpiece interface may cause vibrations leading to poor surface quality. Starting from the analysis of process-machine interaction according to self-excited vibrations theories (the most relevant), this paper outlines a path for surface grinding machines design, focused on the identification of the most critical dynamic eigenmodes both in terms of dynamical parameters and geometry (vibration direction). The methodology is based on the application of Nyquist stability criterion for MIMO systems. Firstly, the methodology distinguishes between a limitation mainly ascribable to regenerative chatter and one ascribable to closed-loop eigenmodes properties. In this latter case, it will be shown that stability properties are strongly influenced by the shape and orientation of the elliptical movement of the wheel entailed by the limiting eigenmode (that, in general, is complex). Such an analysis can be also exploited to provide some indications guiding machine structural modifications. Finally, the approach is demonstrated on a couple of grinding machine variants via FE modeling.

Selection and peer-review under responsibility of the scientific committee of the 6th CIRP Global Web Conference "Envisaging the future manufacturing, design, technologies and systems in innovation era".

Keywords: Grinding, chatter, machine tool design

1. Introduction

Grinding is one of the oldest and most widely used machining process: to date, there are still few alternatives available for producing smooth and flat surfaces, satisfying both technical and economic constraints [1][2]. The quality of a workpiece resulting from a grinding process is strongly influenced by the static and dynamic behavior of the mechanical system, composed by machine tool, wheel, fixture and workpiece. In particular, the dynamic compliance may cause vibrations leading to poor surface quality. For these reason, the comprehension and modelling of grinding process dynamics assume a paramount importance for both end-users and grinder manufacturers [3].

The evolution of design criteria for grinding machines is driven by functional requirements, general trends in machine tools, and cost. The primary functional requirements, as named by Möhring et al. [4], are similar for all machine tools: high static and dynamic stiffness, fatigue strength, damping, thermal and long term stability, low weight for moving parts. Anyway, an effective design approach should take into account the specificity of the particular process in a holistic

Selection and peer-review under responsibility of the scientific committee of the 6th CIRP Global Web Conference "Envisaging the future manufacturing, design, technologies and systems in innovation era".
10.1016/j.procir.2018.09.070

perspective. Recently, dealing with milling process, a design procedure has been proposed based on modeling the interactions between process and machine by means of a stability model of the milling process in modal coordinates [5]. The model allows the identification of the mechanical design parameters that limit the productivity as well as the threshold values that must be met to ensure the targeted productivity. On the same line, in [6] the authors outline a method to traduce the specifications in terms of cutting process in requirements for machine tool dynamic compliance at tool tip. The outcome is a domain of general-purpose machine tools that fit the production requirements from both the dynamic and static point of view.

Dealing with grinding machines, the stability analysis proposed in [7] suggests that grinding machine performance can depend on particular structural properties of the dynamic compliance at wheel hub. It establishes a necessary condition stating that instability can occur only if the vibration direction is comprised between the feed direction and a particular angle depending on grinding force direction. The sufficient condition is a sub-interval whose extent depends on system damping and grinding severity. The instability condition represents a useful indication for a process-aware machine design, suggesting optimal geometrical properties for the dominant structural mode shapes that move the wheel.

The present article moves from these premises to provide a comprehensive analysis of grinding dynamics to point out how the dominant closed loop eigenmodes (machine + process) are affecting machine stability. The approach considers both regenerative phenomenon and force-field instability. In case of force-field instability, this work extend the treatment presented in [7], where only a 1DoF dynamics was considered. In fact, when dealing with real dynamics, the closed loop eigenmodes are generally complex, entailing an elliptical displacement of the wheel. The eigenmodes properties are traced back to machine structural properties that the designer can take into account for machine design modifications.

The article is structure as follows. In section 2, the grinding force model, together with machine-process dynamical interaction and stability assessment via Nyquist criterion is presented. The Section 3 develops the stability analysis distinguishing between regenerative chatter problems or force-field instability and, in this latter case, ascribing the instability onset to particular properties of the close-loop eigenmodes. In Section 4 the methodology is applied to a model of surface grinding machine. Section 5 reports discussion and conclusions.

2. Grinding model

2.1. Force model

In most of the literature, the grinding power is assumed a monotonic function of the Material Removal Rate (MRR) [1]. Then, the tangential grinding force associated to that power can be determined by knowing wheel velocity, while the normal component is usually considered proportional to the tangential one. These components are expressed with respect to a reference frame located at the ideal contact point between the wheel and the workpiece. In case of surface grinding, the tangent component is directed like the feed velocity V_w (that typically is given by the workpiece speed), while the normal direction is orthogonal to the workpiece plane (see Fig. 1).

Mathematically,

$$\begin{Bmatrix} f_x \\ f_y \end{Bmatrix} = b \cdot k_t \begin{Bmatrix} \operatorname{sgn}\Omega \\ \mu \end{Bmatrix} \cdot \left(\frac{MRR}{V_s} \right) \tag{1}$$

with f_x and f_y tangential and normal force component respectively, b width of cut, k_t the tangential cutting coefficient, sgnΩ, V_s the peripheral wheel velocity, μ is f_x/f_y ratio and MRR the Material Removal Rate.

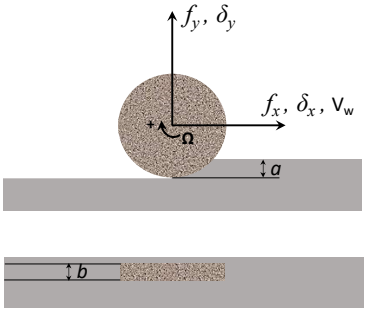

Fig. 1. Grinding parameters definition.

Linearizing the Eq.(1) w.r.t. small change in *MRR* [7], it yields:

$$\mathbf{f} = \begin{Bmatrix} \delta f_x \\ \delta f_y \end{Bmatrix} = \mathbf{f}_{vel} + \mathbf{f}_{pos} = \mathbf{P}_{vel} \begin{Bmatrix} \delta \dot{x} \\ \delta \dot{y} \end{Bmatrix} + \mathbf{P}_{pos} \begin{Bmatrix} \delta x \\ \delta y \end{Bmatrix} \tag{2}$$

with

$$\mathbf{P}_{pos} := \frac{b k_t V_w}{V_s} \begin{bmatrix} 0 & \operatorname{sgn}\Omega \\ 0 & \mu \end{bmatrix}; \quad \mathbf{P}_{vel} := \frac{b k_t}{V_s} \begin{bmatrix} a \operatorname{sgn}\Omega & \operatorname{sgn}\Omega \sqrt{a D_{eq}} \\ \mu a & \mu \sqrt{a D_{eq}} \end{bmatrix}$$

where D_{eq} is the equivalent diameter [1], a the infeed (in case of surface grinding it coincides with the wheel diameter) δx and δy small displacements in tangential and normal direction respectively.

2.2. Grinding dynamics

Grinding dynamics can be effectively represented by the block diagram depicted in Fig. 2, which includes wheel regeneration mechanism. The parameters influencing regenerative mechanism are the wheel rotation period (denoted with τ) and the one-turn radial grinding ratio G_r. This latter defined as $(V_w/V_s)G$, where G is the usual volumetric grinding ratio [1]. The displacements in tangential and normal directions are firstly perturbed by the vibrations induced by grinding force on the wheel-workpiece relative dynamics (represented by the compliance matrix $\mathbf{H}(\omega)$) and wheel compliance ($1/k_c$). Then, the sole displacement in normal direction (that it is assumed to coincide with the infeed direction) is modulated by wheel wear, which decreases the actual infeed. Whereas grinding force is proportional to *MRR*, infeed modulation and infeed rate modulate force as well, that

may increase the vibration level leading the system to instability.

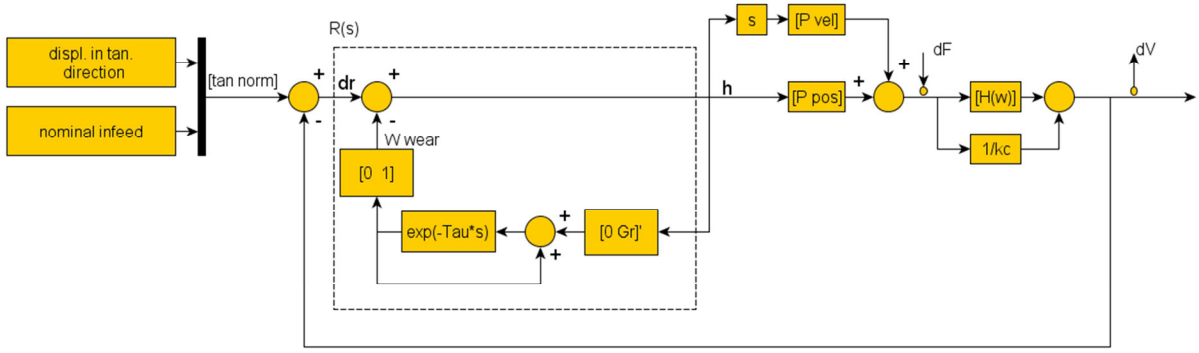

Fig. 2. Block diagram of the grinding wheel regenerative chatter.

The open loop transfer function matrix, denoted by $\mathbf{L}(s,\tau)$, becomes:

$$\mathbf{L}(s,\tau) := \mathbf{R}(s,\tau)\left(\mathbf{P}_{pos} + s\mathbf{P}_{vel}\right)\mathbf{H}(s) \tag{3}$$

where s is the laplacian variable and $\mathbf{R}(s,\tau)$ is the sub-transfer function of the regeneration loop that assumes the form:

$$\mathrm{R}(s,\tau) := \frac{h(s)}{dr(s)} = \left(I + \begin{Bmatrix} 0 \\ G_R \end{Bmatrix} \left(\frac{e^{-\tau S}}{1-e^{-\tau S}} \right) \begin{Bmatrix} 0 & 1 \end{Bmatrix} \right)^{-1} \tag{4}$$

According to the Nyquist criterion for Multi-Input Multi-Output (MIMO) systems, instability occurs when $\det(\mathbf{L}(\omega|\tau)+\mathbf{I})$, traced for the usual D-contour, makes at least one clockwise circle around the origin. In other terms, if there exists a frequency ω such that $\arg(\det(\mathbf{L}(\omega,\tau)+\mathbf{I}) < 180\ °$, the system is unstable. Consequently, the stability limit is traced by the solution of the following equation:

$$\det\left(\mathbf{I}+\mathbf{L}(\omega,\tau)\right) = 0 \tag{5}$$

3. Design criteria

The efficacy of design parameters modification depends on the specific instability phenomenon that must be tackled. Therefore, the first step is aimed at distinguishing the nature of the most critical stability source, according to the model provided in Section 2.

Let the gain $k_a(\omega,\tau)$ be the solution of the stability limit equation derived by Nyquist criterion of Eq.(5), i.e.:

$$k_a = k_a(\omega,\tau) : \det\left(\mathbf{I}+k_a\cdot\mathbf{L}(\omega,\tau)\right) = 0 \tag{6}$$

Whereas the gain $k_a(\omega,\tau)$ must be real for its physical meaning, the imaginary part $\Im\left(k(\omega,\tau)\right)$ must vanish and $\Im\left(k(\omega,\tau)\right)=0$ can be solved w.r.t. τ and substitute it into the Eq.(6), obtaining:

$$\tau = \tau(\omega) \tag{7}$$

$$k = k(\omega) \in \mathbf{R}^+ \tag{8}$$

Eq.(7) and Eq.(8) trace a parametric curve in k_a-τ plane: such a curve is known as Stability Lobes Diagram (SLD). The overall stability performance of the machine is usually well represented by $k_{a\,\min} := \min k_a(\omega)$, that is the critical process gain along all the possible wheel velocities. This KPI presents the advantage to be independent from process planner decisions about wheel velocity.

In order to distinguish if the overall limitation $k_{a\,\min}$ can be traced back to wheel regenerative chatter or to other kind of instability phenomenon, a new stability limit is computed, pretending to cancel out the regeneration loop by posing $\mathbf{R}(s,\tau)=\mathbf{I}$. On this premise, the stability limit equation becomes:

$$k_b = k_b(\omega) : \det\left(\mathbf{I}+k_b\cdot\hat{\mathbf{L}}(\omega)\right) = 0 \tag{9}$$

with $\hat{\mathbf{L}}(\omega) := \left(\mathbf{P}_{pos} + s\mathbf{P}_{vel}\right)\mathbf{H}(\omega)$.

Analogously to $k_{a\,\min}$, the limiting gain $k_{b\,\min} := \min k_b(\omega)$ can be defined. Now, the ratio

$$Q := \frac{k_{a\,\min}}{k_{b\,\min}} \in [1,0] \tag{10}$$

can be used to measure how much instability is due to regenerative phenomenon w.r.t. force field dynamical properties. If $Q\to 1$, the effect of regeneration exclusion is negligible, meaning that regeneration does not have a significant effect. If $Q\to 0$, the stability limit without regeneration is extremely high (virtually, not existing), meaning that the regeneration mechanism is dominating chatter occurrence.

Let the case $Q\to 1$ be considered. In this case, the instability is due to a particular properties of the process force field, which is not conservative and allows closed path integrals associated to energy accumulation. In other words,

$$W_{TOT} = \oint_{\Gamma,\dot{\Gamma}} \mathbf{f}\cdot d\mathbf{p} \tag{11}$$

where $\mathbf{p}$ is the generic position vector, Γ a generic path and $\dot{\Gamma}$ the velocity on the path.

The energy of Eq.(11) can be explicitly computed considering the motion associated to the eigenmode of the

closed loop system at stability limit (hereafter denoted by $\boldsymbol{\phi}:=\{\phi_x \;\; \phi_y\}$). This eigenmode corresponds to the null eigenvalue entailed by Eq.(9) at a given chatter frequency ω_c. In time domain, this motion becomes:

$$\mathbf{p}(t) \equiv \begin{cases} x = |\phi_x| \cos(\omega_c t + \alpha_x) \\ y = |\phi_y| \cos(\omega_c t + \alpha_y) \end{cases} \tag{12}$$

with $\alpha_x = \arg(\phi_x)$, $\alpha_y = \arg(\phi_y)$ and

The Eq.(12) corresponds to an ellipse expressed in parametric form. Canceling out the temporal parameter, the ellipse equation assumes the usual form:

$$Ax^2 + Bxy + Cy^2 = 1 \tag{13}$$

with

$$A := \frac{1}{|\phi_x|^2 \sin(\alpha_y - \alpha_x)}; \; B := \frac{-2}{|\phi_x||\phi_x| \tan(\alpha_y - \alpha_x)};$$
$$C := \frac{1}{|\phi_y|^2 \sin(\alpha_y - \alpha_x)};$$

The ellipse of Eq.(13) is centered in the origin and its principal axes are rotated by an angle β w.r.t. to the reference frame xy (see Fig. 3). The rotation angle β can be computed as follows:

$$\beta = \tan^{-1}\left(\frac{C - A + \sqrt{(C-A)^2 + B^2}}{B}\right) \tag{14}$$

while the length of the principal axes A_I and A_J is given by the following expressions:

$$A_I = \sqrt{\frac{1}{a\cos^2\beta + b\cos\beta\sin\beta + c\sin^2\beta}}; \qquad A_J = \sqrt{\frac{1}{a\sin^2\beta + b\cos\beta\sin\beta + \cos^2\beta}} \tag{15}$$

Then, Eq.(12) can be rewritten as follows:

$$\mathbf{p}(t) = \begin{Bmatrix} x \\ y \end{Bmatrix} = \begin{bmatrix} \cos\beta & -\sin\beta \\ \sin\beta & \cos\beta \end{bmatrix} \begin{Bmatrix} A_I \cos\omega_c t \\ A_J \sin\omega_c t \end{Bmatrix} \tag{16}$$

Let, now, Eq.(11) be analyzed. The overall energy W_{TOT} transferred by the process to the machine can be decomposed into two parts: W_{pos} (depending on the positional component of the process force field $\mathbf{f}_{pos}$) and W_{vel} (depending on the velocity-dependent component $\mathbf{f}_{vel}$). Namely, the Eq.(11) can be rewritten as follows:

$$W_{TOT} := W_{pos} + W_{vel} = \oint_\Gamma \mathbf{f}_{pos} \cdot d\mathbf{p} + \int_0^{\frac{2\pi}{\omega_c}} \mathbf{f}_{vel} \cdot \dot{\mathbf{p}} dt = \oint_\Gamma \mathbf{P}_{pos}\mathbf{p} \cdot d\mathbf{p} + \int_0^{\frac{2\pi}{\omega_c}} \mathbf{P}_{vel}\dot{\mathbf{p}} \cdot \dot{\mathbf{p}} dt \tag{17}$$

where Γ becomes the closed path of the limit cycle associated to the asymptotic stability at stability limit, that in our case is the ellipse of Eq.(16), properly scaled by a factor δ (i.e., $\delta \cdot \mathbf{p}(t)$) and ω_c the corresponding frequency.

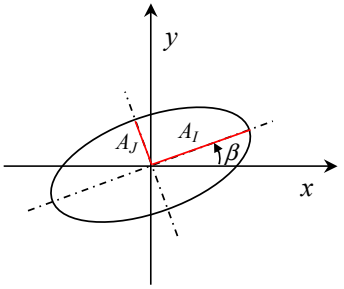

Fig. 3. Rotated ellipse.

Whereas the term W_{pos} is given by the circulation of a positional force field over the space domain, the Kelvin-Stokes theorem can be applied, stating:

$$\oint_\Gamma \mathbf{P}_{pos}\mathbf{p} \cdot d\mathbf{p} = \iint_S \nabla\times(\mathbf{P}_{pos}\mathbf{p}) dA = \nabla\times(\mathbf{P}_{pos}\mathbf{p}) A \tag{18}$$

where $\nabla\times$ is the vector field curl and A the area of the surface S delimited by the closed path Γ. It can be noted that for linear positional forces, curl operator is constant. Therefore, substituting $\mathbf{P}_{pos}$ and A expressions into Eq.(18), it yields:

$$W_{pos} = \delta\pi A_I A_J \frac{bk_t V_w}{V_s} \operatorname{sgn}\Omega \tag{19}$$

Provided that all the terms except $\operatorname{sgn}\Omega$ and $A_{I/J}$ are positive by definition, it can be noted that there exists energy injection if and only if $A_I A_J \operatorname{sgn}\Omega < 0$. This condition implies that wheel center trajectory is someway "orbital".

On the other side, substituting $\mathbf{P}_{vel}$ expression into W_{vel} with the same previous elliptical path, it yields:

$$W_{vel} = -\frac{bk_t}{V_s}\left(C(\beta) + C_I\right)\omega\pi\delta \tag{20}$$

with

$$C(\beta) := (A_I + A_J)(A_I - A_J)\left(\mu\sqrt{aD_{eq}} - a\operatorname{sgn}\Omega\right)\cos^2\beta + -\left(\sqrt{aD_{eq}}\operatorname{sgn}\Omega + \mu a\right)(A_I + A_J)(A_I - A_J)\sin\beta\cos\beta$$

and $C_I := -{A_I}^2\mu\sqrt{aD_{eq}} - {A_J}^2 a\operatorname{sgn}\Omega$

The Eq.(20) shows that W_{vel} can be decomposed into two distinct components: one dependent on the angle β (proportional to $C(\beta)$) and one independent (proportional to C_I). Obviously, when A_I=A_J, the effect of β vanishes, because the ellipse becomes a circle and β does not affect oscillation path geometry.

In Fig. 4, the overall energy W_{TOT} is plotted (by color scale) w.r.t. β and A_J for δ=A_I=1, for the process parameters of the chatter frequency reported in Table 1. Due to the unitary A_I, the A_J axis can be interpreted as the ratio A_J/ A_I that goes to 0 when the elliptical orbit collapses on a straight line. The only possibility to incur in instability is when W_{TOT} is negative, namely, when the process injects energy into the system. Otherwise, the process is dissipative and tends to damp vibrations. The magenta line of Fig. 4 represents the border of such necessary condition: (A_J,β) pairs falling inside the ellipse can lead to instability if the energy injected by the process is greater than the energy dissipated by the structure. This result agrees with that one obtained in [7], which represents the section of the surface $W_{TOT}(A_J, \beta)$ for A_J=0.

Table 1. Process parameters

k_t	b	V_w	Ω	D_w	G	a	μ	f_c
[J/mm^3]	[mm]	[m/s]	[rpm]	[m]		[mm]		Hz
30	1	0.53	-1000	600	2.6	0.01	1.4	86

In Fig. 4, the necessary condition border is drawn also for other different process parameters. It can be noted how the border is surprisingly insensitive to infeed and feed velocity, while it strongly depends of the μ ratio (confirming the results obtained in [7]).

The dependency of the necessary condition border on β and A_J/A_I is the key to suggest which characteristics the closed loop limiting eigenmode has to exhibit to ensure grinding stability.

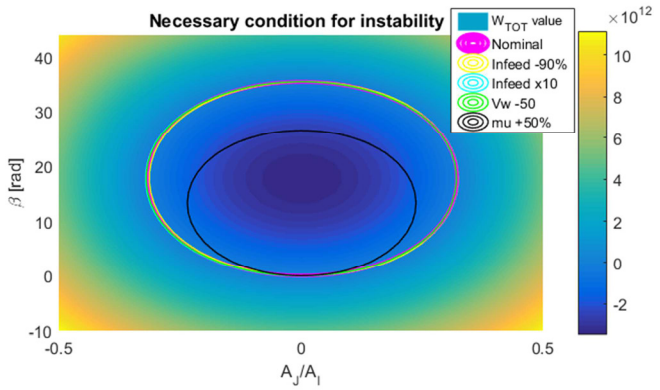

Fig. 4. Normalized Total cycle energy (W_{TOT}).

4. Application example

The outlined approach is applied to the design of a large surface grinding machine with a gantry architecture (Fig. 5). Machine strokes specifications are 5500mm for the longitudinal axis X, 2000mm for the traverse axis Y and 1025mm for the vertical axis Z. The spindle is supposed to be equipped with an Aluminium Oxide wheel (dimension: 610x100x127) that weighs about 60Kg. A FE model of the first design variant has been built and the dynamic compliances at wheel hub computed (see Fig. 6).

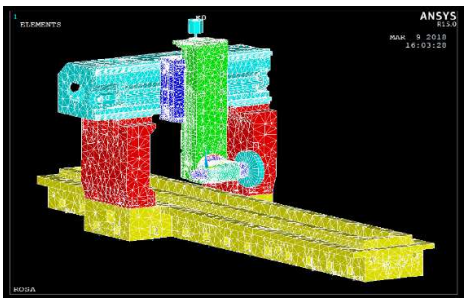

Fig. 5. FE model of the sample grinding machine.

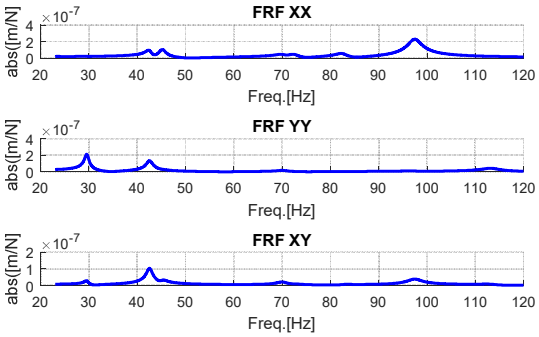

Fig. 6. FRFs at wheel hub.

Applying the methodology exposed in Section 3, with the process parameters of Table 1, the k_a and k_b have been computed. For sake of clarity, the SLD and the "flatted" SLD due to regenerative loop elimination are depicted in Fig. 7 (a) and (b) respectively.

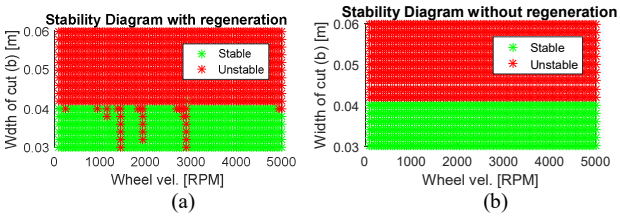

Fig. 7. SLD (a) and "flattened" SLD (b).

It yields Q=0.75, meaning that regeneration mechanism is not the main concern for instability (as evident from the figures).

Getting a reduce analytical representation of FEM dynamics and coupling it with the grinding process model without the regenerative loop (i.e., $\hat{\mathbf{L}}(s)$), it is possible to compute the closed loop poles of the system for different grinding parameters combinations. In Fig. 8, the maximum real part among the overall poles is represented w.r.t. width of cut and infeed: the red line, corresponding to a null value, represents the stability limit.

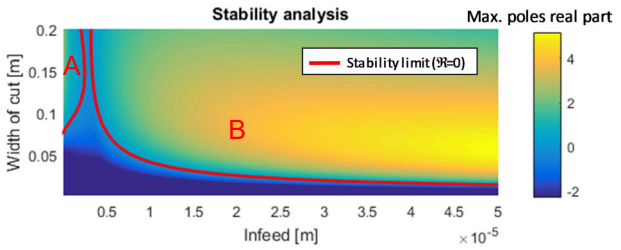

Fig. 8. Stability analysis w.r.t. width-of-cut and infeed

In case of unstable cutting combinations, the eigenmode associated to the most critical pole (whose real part is plotted in Fig. 8) can be computed. The corresponding β angle and A_J/A_I are depicted in Fig. 9 with the indications (by color) of the absolute value of the negative relative damping, which measures the vibration growth rate, and the instability necessary condition border.

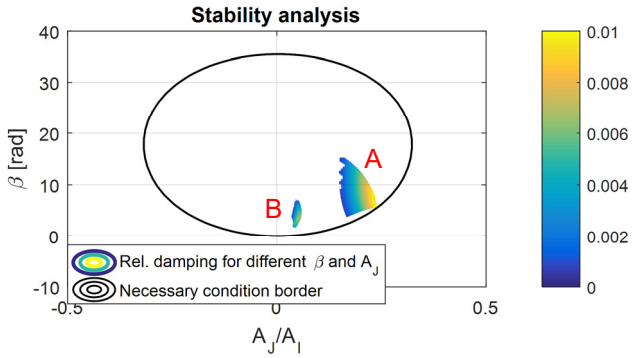

Fig. 9. Unstable β and A_J/A_I combitation with vibration growth rate

In the most critical zone, where the majority of grinding operations fall (i.e. where a>1μm), β is around 5 deg, while A_J/A_I is around 0.07: the closed loop eigenmode entails a nearly straight trajectory that, according to the necessary condition of Fig. 4, can lead to instability. In the region where a<1μm, the instable region entails higher A_J/A_I (around 0.12) and higher β (around 10 deg): in fact, according to necessary condition locus, higher A_J/A_I needs higher β to fall into instability.

Considering that, near the stability limit, the angle β has almost the same value independently from the infeed, it can be stated that the process coupling does not affect eigenmode geometry. Hence, the closed loop eigenmode is assumed to be similar to the open loop one, i.e., the eigenmode that the designer can control by the proper structural modification.

Root locus analysis highlights that the critical eigenmode is associated to a resonance at about 97Hz. Consequently, it can be stated that a good strategy for increasing machine stability property is to change the structure in order to get the structural eigenmode at 97Hz more "horizontal", or rather "vertical" (i.e. β>35°). The first solution weakly depends on μ value, while the second strongly depends on it, as shown in Fig. 4. A complementary strategy would consist in increasing eigenmode complexity, in order to obtain a more "orbital" vibrational trajectory of the wheel hub; but this latter criterion can be hardly traced back to design modification, since it involves reasoning about structural and lumped damping, which is notoriously uncertain.

5. Conclusions

This article presents a stability analysis for grinding operations that relates the stability characteristics of the process to the geometrical properties of the eigenmodes of the closed loop machine-process system. In case regenerative phenomenon can be neglected, a necessary condition for instability has been identified, expressed in terms of principal axes ratio and inclination the elliptical trajectory associated to the most critical eigenmode. It is worthwhile to be noted that such a necessary condition depends only on the ratio between normal and tangential grinding force (as already pointed out in [7] for a special case). Whereas the closed loop and open loop critical eigenmode are similar, the indications about its optimal characteristics can guide the designer to the proper structural modifications.

References

[1] Rowe WB. Principles of Modern Grinding Technology. 2nd ed. Waltham (U.S.): William Andrew (Elsevier); 2014.
[2] Wegener K, Bleicher F, Krajnik P, Hoffmeister HW, Brecher C. Recent developments in grinding machines. CIRP Ann - Manuf. Technol 2017; 66:779–802.
[3] Leonesio M, Parenti P, Cassinari A, Bianchi G, Monno M. A Time-Domain Surface Grinding Model for Dynamic Simulation. Procedia CIRP 2012; 4:166–171.
[4] Möhring HC, Brecher C, Abele E, Fleischer J, Bleicher F. Materials in Machine Tool Structures. CIRP Ann - Manuf Technol 2015; 64(2): 725–748.
[5] Zulaika JJ, Campa FJ, Lopez de Lacalle LN. An integrated process–machine approach for designing productive and lightweight milling machines. Int J Mach Tools Manuf 2011; 51:591–604.
[6] Leonesio M, Molinari Tosatti L, Pellegrinelli S, Valente A. An integrated approach to support the joint design of machine tools and process planning, CIRP J Manuf Sci Technol 2013; 6:181–186.
[7] Leonesio M, Parenti P, Cassinari A, Bianchi G. Force-field instability in surface grinding. Int J Adv Manuf Technol 2014; 72:1347–1360.